DELAYED CURVATURES IN POROUS CERAMIC WALL TILES

[1] V. Cantavella, [1] A. Moreno, [1] A. Mezquita, [1] F. Gilabert, [2] J. Barber, [2] A. Palanques

[1] Instituto de Tecnología Cerámica (ITC). Asociación de Investigación de las Industrias Cerámicas (AICE)
Universitat Jaume I. Castellón. Spain
[2] Cerámica Saloni, S.A. San Juan de Moró. Spain

ABSTRACT

This study analyses the factors that affect delayed curvatures in porous ceramic wall tiles. The study was conducted on two industrial white-body earthenware wall tile models, size 600x300 mm, which displayed different delayed curvatures. Tiles from the two models were fired under industrial conditions, and the evolution of the curvature was determined over a period of 60 days. A complete mechanical characterisation of these tiles was also conducted.

Finally, a model was developed that enabled the evolution of curvature with time to be estimated, and the mechanisms through which curvature is produced to be understood. The values provided by the model agree very well with the experimental data throughout the entire analysed period of time.

1. INTRODUCTION

Delayed curvatures are the curvatures that change after tiles have left the kiln. This phenomenon is particularly pronounced in the case of porous ceramic wall tiles and porcelain tile, though the change in curvature is qualitatively different in the two types of products. In wall tiles, the evolution is usually towards concavity (this is one of the reasons why it is sought to provide the pieces with a slightly convex curvature at the kiln exit), while porcelain tiles tend, first, to evolve towards concavity and then towards convexity [1].

In principle, there are few factors could produce delayed curvatures: expansion of the body, residual stresses, and creep (non-elastic behaviour of the bodies), though there are many that could, indirectly, change them: thickness of the body, engobe, and glaze, moduli of elasticity, heating and cooling rate, coefficients of linear expansion of the layers, apparent porosity, etc. Delayed curvatures therefore constitute a complex problem under industrial conditions.

To the above, it should be added that delayed curvatures develop over long periods of time, which may involve a week or more. This prevents immediate remedial adjustments from being made in the process, unlike what occurs with immediate curvatures (i.e. those that the tile displays at the kiln exit).

2. MEASUREMENT OF DELAYED CURVATURE

In order to analyse the problem of delayed curvatures, two white-body earthenware wall tile models, each measuring 600 x 300 mm, were selected:

- Model A: Tiles with a glossy glaze application. These exhibited noticeable delayed curvature.
- Model B: Tiles with a matt glaze application. These displayed significantly smaller delayed curvature than that of model A.

Tiles of the two models were fired under industrial conditions to a peak temperature of 1150 ºC, in a 65-min cycle. After the tiles had left the kiln, their delayed curvature was measured over a period of 2 months, analysing 5 tiles of each model. The results obtained are shown in figure 1. The initial tile curvature (at zero time) cannot be represented on a logarithmic scale, so that it is shown as a horizontal segment.

It may be observed how, in both cases, the end curvature is practically the same (slightly less than 0.5 mm), though the initial curvatures are quite different (2.07 and 1.45 mm for models A and B, respectively). The figure also shows that the relationship between curvature and the logarithm of time is practically linear in the analysed range, which goes from 2 hours to 2 months after firing.

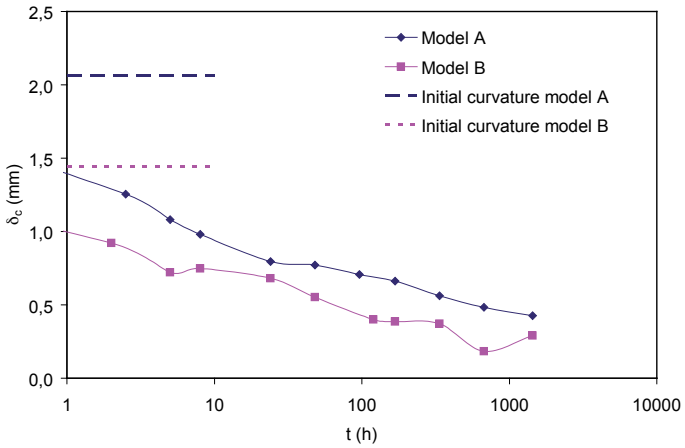

Figure 1. Evolution of the delayed curvature of model A and B tiles.

3. CHARACTERISATION

3.1. Modulus of elasticity.

The body modulus of elasticity can be readily determined by a tensile test. The glaze modulus of elasticity, if the glaze is homogeneous, can be measured using indentation tests. The engobe poses greater difficulties, however, since engobe porosity makes it difficult to obtain precise results by indentation while, on the other hand, if an engobe test piece were to be formed that could be subjected to a bending test, this could lead to different properties from those of a thin engobe layer.

In order to address these difficulties, test pieces were prepared with a fixed layer thickness of the body (h_s=7.56 mm), and a variable layer thickness of the engobe (h_g=0 / 160 / 349 / 539 μm) and of the glaze (h_v=328 / 692 / 776 μm), and the effective modulus of elasticity (E_{ef}) of the test pieces was determined. E_{ef} is the modulus that a homogeneous piece would have, of the same dimensions, which displayed the same load/displacement curve as the tested piece. E_{ef} can be related to the thickness of the engobe and glaze layers, as well as to their moduli of elasticity, yielding:

$$\frac{E_{ef}}{E_s} = \frac{4}{(1+h'_g+h'_v)^3}\begin{bmatrix}(1-E'_g)(1-z'_0)^3+\\+(E'_g-E'_v)(1+h'_g-z'_0)^3+\\+z'^3_0+E'_v(1+h'_g+h'_v-z'_0)^3\end{bmatrix}$$

Equation 1.

$$z'_0 = 1+\frac{E'_g h'^2_g + E'_v h'_v(2h'_g+h'_v)-1}{2(E'_g h'_g + E'_v h'_v+1)}$$

Equation 2.

The meaning of the parameters that appear in the foregoing equations are given in section 6.

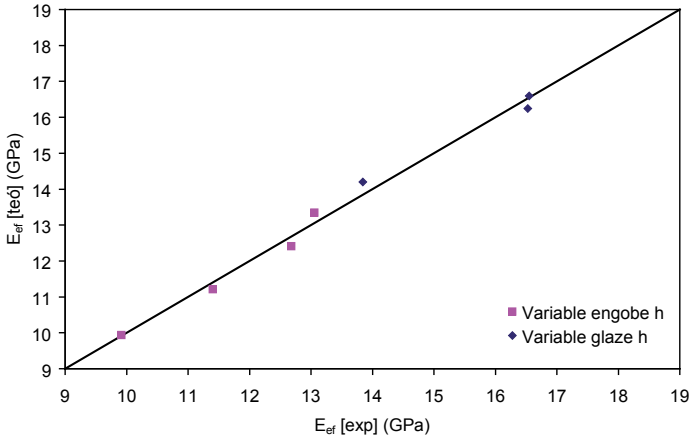

Figure 2. Plot of the theoretical modulus of elasticity (equation 1) as a function of the experimental modulus of elasticity.

The theoretical modulus of elasticity (calculated using equation 1) is plotted as a function of the experimental modulus of elasticity, for the tests conducted with different engobe and glaze thicknesses of model A, in figure 2. Good agreement can be observed between the theoretical and the experimental values. This fit was used to determine the moduli of elasticity shown in table 1.

E_s (MPa)	9.93
E_g (MPa)	32.4
E_v (MPa)	34.7

Table 1. Moduli of elasticity of the different layers.

3.2. Creep.

Creep consists of the strain of a material under the application of a constant load [2, 3]. An irreversible process is therefore involved. In order to quantify creep, the device shown in figure 3 was used, which enables a constant load to be applied by means of a series of weights, and the evolution of strain to be recorded as a function of time.

Figure 4 shows the strain deflection for all the analysed body test pieces, as well as the value fitted to the semi-empirical equation:

$$w = A\left[1-\exp\left(-\left(\frac{t}{\tau}\right)^{\beta}\right)\right]+\frac{FS^3}{12b\eta h^3}t$$

Equation 3.

A, τ and β are empirical fitting parameters. The meaning of the other parameters is given in section 6.

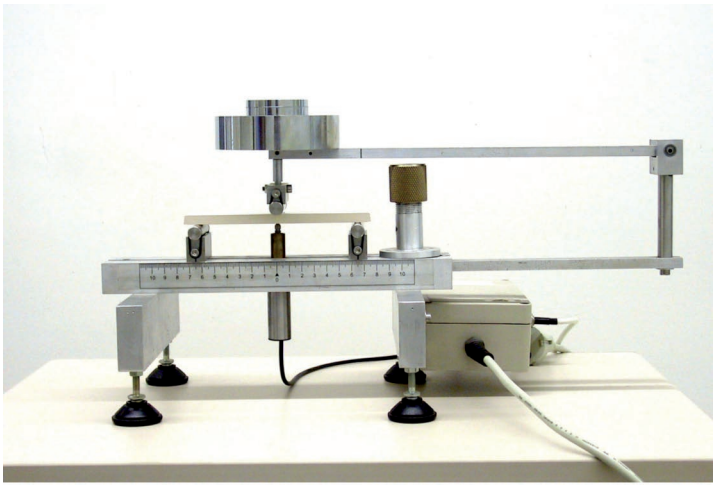

Figure 3. Device used to measure creep in ceramic test pieces.

The above procedure can also be applied to determine the creep parameters of the engobe and glaze, using glazed test pieces; in this case, however, the resulting deflection value corresponds to the creep of the body and to that of the layers to be analysed. Since the thickness of the engobe and the glaze layers is relatively small, and the scatter in the body flow curves is high (figure 4), it may be concluded that the creep parameters of the engobe and glaze are going to exhibit a great uncertainty.

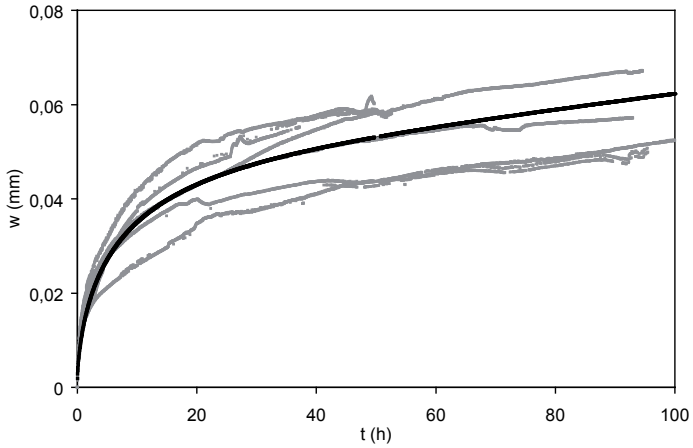

Figure 4. Evolution of deflection as a function of time in several test pieces. The darkest curve corresponds to the fit.

In any event, the experiments conducted indicated that the engobe and glaze creep had to be negligible compared with that of the body. To verify this finding, experiments were conducted in which several glazed test pieces were subjected to creep tests with the glazed surface facing upwards (body under tension) or facing downwards (body under compression). The results, shown in figure 5, indicate that when the body is under tension, the creep is very high, whereas when it is under compression, the creep is practically negligible. The most likely explanation is that the creep in the body is due to a series of microcracks that can open (figure 6).

If the body is under tension, the opening of the microcracks leads to strain that is interpreted as creep; in contrast, if the body is under compression, since the cracks cannot close, no appreciable strain occurs. If the glaze displayed creep when the glazed surface was facing downwards, the strain would be greater.

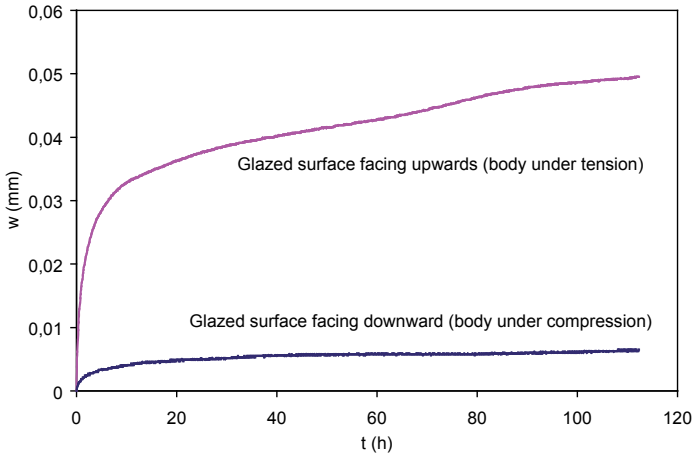

Figure 5. Strain deflection by creep of glazed, test pieces with the glazed surface facing upwards or downwards.

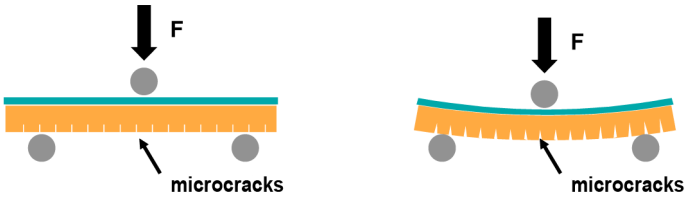

Figure 6. Proposed mechanism for explaining creep in bodies.

3.3. Residual stresses.

There are two types of residual stresses, and both are generated during cooling:

- Stresses caused by thermal gradients: These occur in the body owing to thermal differences between the surface and the centre.
- Stresses resulting from the glaze-body fit: These develop owing to differences in the coefficients of linear expansion of the different layers.

3.3.1. Stresses caused by thermal gradients.

The stresses caused by thermal gradients in earthenware wall tiles were analysed elsewhere [4], it being observed that the profiles of these stresses depended markedly on the cooling rate, while all the analysed cases yielded symmetrical profiles.

The stress profiles can relax with time due to creep; if they are symmetrical, however, their relaxation does not lead to curvatures. Therefore, in a first approach it should not be necessary to take them into account in order to explain the curvatures.

3.3.2. Stresses resulting from the glaze-body fit.

One of the most widely used methods for measuring the stresses arising from the glaze-body fit is the Steger method [5]; however, this method is qualitative and does not allow the deflection strain (test result) to be related to the value of the stresses in the glaze.

A procedure was devised to determine the residual stresses. The method consisted of the measurement of the modulus of rupture (effective mechanical strength) of test pieces of body, body+engobe, and body+engobe+glaze. Using the elasticity equations, a function can be established of the following form:

$$\Delta\sigma_R = f(\Delta\varepsilon_{fg}, \Delta\varepsilon_{fv})$$

Equation 4.

where ($\Delta\sigma_R$) is the change in the modulus of rupture when an engobe layer or an engobe+glaze layer is added to a body, and $\Delta\varepsilon_{fg}$ and $\Delta\varepsilon_{fv}$, are the differences in expansion between the body, engobe, and glaze layers. $\Delta\varepsilon_{fv}$ is numerically equal to the difference in shrinkage between the glaze and the body, with a changed sign, customarily represented by Δc. The difference Δc is usually calculated from the body/glaze fit theory, by the superposition of the dilatometric curves of the two layers [6]. Equation 4 is, therefore, an alternative method of obtaining Δc, which, in addition, can also be applied to the fit between the engobe and the body. Finally, the two values of $\Delta\varepsilon_f$ enable the stresses in the body, engobe, and glaze to be quantified.

Table 2 details the effective mechanical strength of the different analysed pieces (σ_R), as well as the values of $\Delta\varepsilon_{fg}$ and $\Delta\varepsilon_{fv}$ and the residual stresses in the area of the body close to the engobe ($\sigma_{s,up}$), and in the glaze layer ($\sigma_{v,up}$). It may be noted that the positive stress values correspond to tensile stresses and the negative stress values to compressive stresses; therefore, according to table 2, the body is under tension and the glaze is under compression.

σ_R (MPa)	body	15.99
	body + engobe	16.99
	body + engobe + glaze	20.33
$\Delta\varepsilon_{fg}$ • 1000		-0.01
$\Delta\varepsilon_{fv}$ • 1000		0.79
$\sigma_{s,up}$ (MPa)		2.27
$\sigma_{v,up}$ (MPa)		-24.9

Table 2. Data used to calculate the residual stresses caused by the fit.

3.4. Body expansion.

3.4.1. Discontinuous measurement.

In order to measure the expansion of the bodies, their dimensions were determined using a coordinate measurement apparatus. This apparatus has a precision of about 1 μm, the repositioning error of the piece itself being greater because the measurements were made discontinuously.

Expansion measurements were carried out on bodies fired under industrial conditions. The result obtained is shown in figure 7. The first measurement was made two hours after the body had left the kiln; it is therefore not known how expansion evolved before those two hours. It may be observed that there is a practically linear relationship between the expansion of the body and the logarithm of time. This type of relationship has also been found by other authors [7], and it displays similarities with what occurs in delayed curvature (figure 1), which suggests that there is quite a direct relationship between the two magnitudes.

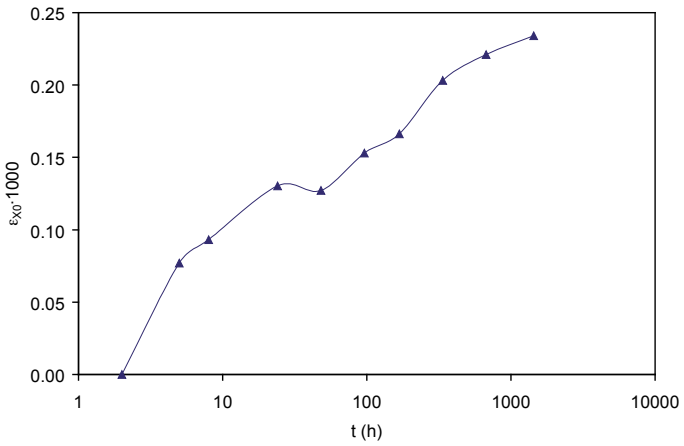

Figure 7. Evolution of body expansion as a function of time.

The main problem in measuring expansion is the impossibility of knowing the initial expansion of the piece. This information is needed if it is sought to explain the initial change in curvature which, as figure 1 shows, is very important.

3.4.2. Measurement of initial expansion.

In order to quantify the initial expansion of the tiles, test pieces were prepared from unfired industrial tiles. After these test pieces had been cut to a size of 150 x 30 mm, they were fired in an electric laboratory kiln to a peak temperature of 1130 ºC, approximately corresponding to the 1150 ºC used in industrial firing. The test pieces were cooled by quenching, the pieces being withdrawn from the kiln at peak temperature and allowed to cool at room temperature. This was intended to simulate the effect of the rapid cooling that occurs in industrial kilns.

The evolution of the expansion during the first 24 hours is depicted in figure 8. It shows that this expansion is even slightly greater than that which occurs in the period from 2 hours to 2 months after firing. Consequently, it cannot be considered negligible.

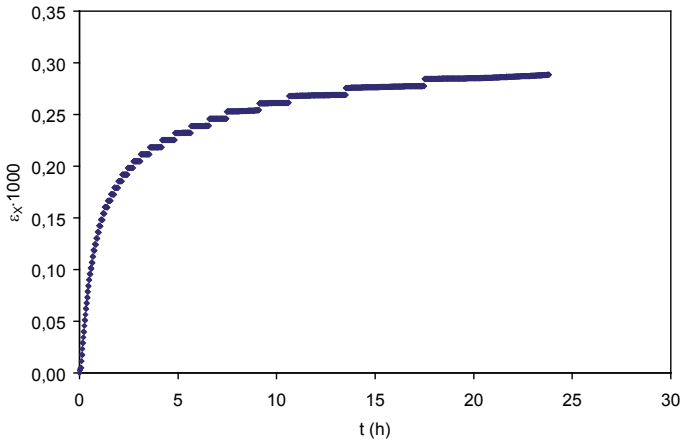

Figure 8. Evolution of body initial expansion as a function of time.

4. MODELLING

4.1. Influence of residual stresses and creep.

A complete mathematical model could be developed to take into account the effect of residual stresses and creep on delayed curvatures. However, a simpler argument can help rule out residual stresses as a cause of the curvatures:

1. As table 2 shows, the stresses in the body, next to the engobe, are tensile stresses. The combination of these stresses and creep would lead to convex tile curvature, which is the opposite of what is experimentally observed. In any event, such residual stresses would lead to opposite curvatures from those that are experimentally noted.
2. The creep tests shown in figures 4 and 5 were performed with loads that produced internal stresses about an order of magnitude higher than the residual stresses; however, they did not cause strains larger than 60 μm. Taking into account the change of scale (the test pieces used in creep were 150 mm long compared with 600 mm of the industrial pieces), and considering a proportionality between stress and strain, the residual stresses+creep could cause a delayed curvature of 0.1 mm, which, in any event, would have an opposite sign to that observed experimentally.

4.2. Influence of moisture expansion.

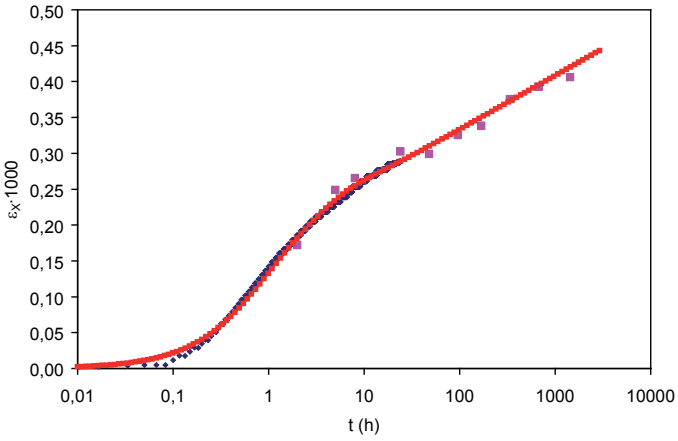

Figure 9. Evolution of body total expansion as a function of time.

The results of the initial expansion (figure 8) and of the expansion measured up to two months after firing (figure 7) can be combined. This yields a series of data that encompass the period from the time the tile leaves the kiln to two months afterwards (figure 9). These data were fitted to an empirical equation of the form:

$$\varepsilon_X = a_1(1-e^{-t/\tau_1}) + a_2(1-e^{-t/\tau_2}) + b_2 \ln(1+t/\tau_2)$$

Equation 5.

where a_1, a_2, τ_1 and τ_2 are constants. Using the elasticity equations, the following relationship between body expansion (ε_X) and curvature (κ) can be established:

$$\kappa = \frac{1}{h}\frac{6(1-2z_0')\varepsilon_X}{(1+h_g'+h_v')^2 E_{ef}'}$$

Equation 6.

Strain deflection can be obtained from curvature (κ), using the expression:

$$\delta_c = \frac{L^2\kappa}{8}$$

Equation 7.

Equations 6 and 7 yield the evolution of the curvature deflection as a function of time. The real curvature of the tile will be the one provided by these equations plus the initial curvature (the curvature displayed by the tile at the kiln exit).

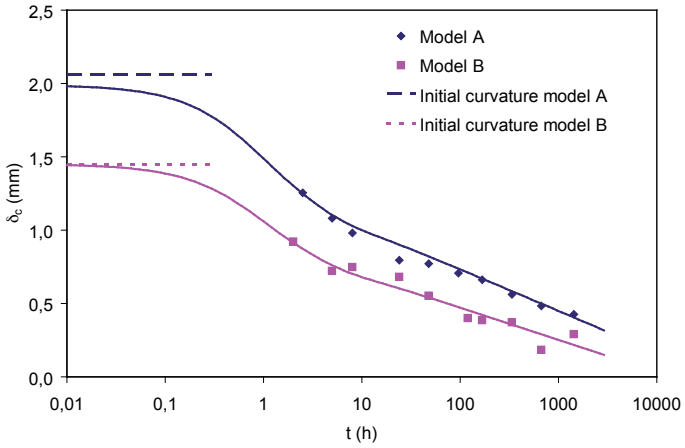

Figure 10. Evolution of theoretical curvature for the analysed models. Comparison with the experimental data.

From these equations, taking into account the initial tile curvature, the results were obtained that are displayed in figure 10, which show good agreement with the experimental data. Therefore, an elastic model that just takes into account tile body expansion is able to explain the evolution of tile curvature with time. Evidently, factors such as the moduli of elasticity or thickness of the different layers influence the particular curvature value, but the *driving force* of the process essentially seems to be body expansion.

5. CONCLUSIONS

- A procedure has been developed that allows the modulus of elasticity in engobe and glaze layers to be measured.
- A method has been established for measuring the residual stresses resulting from the glaze/body fit. This method is based on determining the effective mechanical strength of test pieces of body, body+engobe, and body+engobe+glaze. Compared with the Steger method, the developed method has the advantage of being quantitative.
- The measurement of creep in earthenware wall tile bodies, engobes, and glazes indicates that the tile bodies display a greater creep strain. The creep in tile bodies is possibly related to a microcrack-opening mechanism, though further study is needed to confirm this hypothesis.
- The wall tile bodies analysed display notable expansion. This expansion is rapid, and it has been verified that the dimensional change that occurs during the first 24 hours is greater than that which takes place in the following two months.
- A model based on the elastic behaviour of the tiles (made up of a body, engobe, and glaze) and on the expansion of the tile body has been developed. This model correctly predicts the evolution of delayed curvatures.

- The expansion of the tile bodies seems to be the main cause of the delayed curvatures in earthenware wall tiles.

6. NOMENCLATURE

a_i: Dimensionless constants of the equation for estimating tile body expansion as a function of time. ι may be 1 or 2.

E_c: Modulus of elasticity of layer c, where c may be s (body), g (engobe), or v (glaze) [MPa].

$E_{'c}$: Dimensionless modulus of elasticity: E_c/E_s.

E_{ef}: Effective modulus of elasticity [MPa].

E'_{ef}: Dimensionless effective modulus of elasticity: E_{ef}/E_s.

F: Applied force [N].

h: Total thickness of the test piece [m].

h_c: Thickness of the layer c, where c may be s (body), g (engobe), or v (glaze) [m].

h'_c: Dimensionless thickness: h_c/h_s.

L: Length of the piece [m].

S: Span between supports in the three-point bending test [m].

t: Time [s].

w: Strain deflection in the bending test [m].

z_0: Position of the neutral fibre, measured from the rib surface [m].

z'_0: Dimensionless position of the neutral fibre: z_0/h_s.

β: Empirical exponent in the creep equation.

$\Delta\varepsilon_{fg}$: Difference in expansion between the engobe and the body.

$\Delta\varepsilon_{fv}$: Difference in expansion between the glaze and the body.

δ_c: Curvature deflection [m].

ε_X: Body expansion evaluated from the time the tile leaves the kiln.

ε_{X0}: Body expansion evaluated from a time *t* after the tile has left the kiln.

η: Effective viscosity [Pa·s].

κ: Curvature [m^{-1}].

$\sigma_{s,up}$: Residual stresses in the body, near the engobe [MPa].

$\sigma_{v,up}$: Residual stresses in the glaze [MPa].

τ: Time constant [s].

τ_i: Time constants of the equation for estimating tile body expansion as a function of time. i may be 1 or 2 [s].

REFERENCES

[1] V. Cantavella, J. García-Ten, E. Sánchez, E. Bannier, J. Sánchez, C. Soler, J. Sales. Curvaturas diferidas en gres porcelánico. Análisis y medida de los factores que intervienen. En: Xth World Congress on Ceramic Tile Quality - Qualicer 2008. Castellón: Cámara oficial de comercio, industria y navegación, 2008. pp. P.BC207-P.BC224.

[2] G.W. Scherer Relaxation in glass and composites. New York: John Wiley & Sons, 1986.

[3] W.R. Cannon and T.G. Landon. Review Creep of Ceramics. Part 1 Mecanical characteristics. J.Mater.Sci. 18, 1983, pp. 1-50.

[4]. V. Cantavella, A. Moreno, A. Mezquita, J.C. Jarque, J. Barberá, A. Palanques. Evolución de las tensiones y curvaturas en soportes porosos durante el enfriamiento. En: Xth World Congress on Ceramic Tile Quality - Qualicer 2008. Castellón: Cámara oficial de comercio, industria y navegación, 2008. pp. P.BC241-P.BC255.

[5] J.L. Amorós, A. Blasco, J.V. Carceller, V. Sanz. Acuerdo esmalte-soporte (II). Expansión térmica de soportes y esmaltes cerámicos. Técnica Cerámica, 179, 644-657, 1989.

[6] J.L. Amorós, F. Negre; A. Belda; E. Sánchez. Acuerdo esmalte-soporte (I) Causas y factores de los que depende. Técnica Cerámica, 178, 582-592, 1989.

[7] R.G. Bowman, P.J. Banks. Theoretical modelling of external wall tiling systems. En: www.infotile.com/services/techpapers/33icbest.shtml, 6 p., 2000.